Energy and Power 2013, 3(2): 18-25
DOI: 10.5923/j.ep.20130302.02

Vector Control Analysis of Doubly-Fed Induction Generator in Wind Farms

Hassan Abniki[1,*], Mahmood Abolhasani[2], Mohammad Ehsan Kargahi[1]

[1]ECE School, University of Tehran, Tehran, Iran
[2]Faculty of Environment and Energy, Science and research branch Islamic Azad University, Tehran, Iran

Abstract This paper presents vector control of grid-connected wind turbines; also the second goal of this research is to survey the vector control for wind turbines with doubly-fed induction generators (DFIGs) when a short circuit faults in grid happens. In fact in this paper, vector control of stator-flux is applied for stator- and rotor-side converters in order to control of active and reactive powers simultaneously, and to keep the DC-link voltage constant. Also the method performances are tested in different cases.

Keywords Vector Control, Wind Turbine, DFIG, Inverter

1. Introduction

Nowadays, DFIGs are used by the industry for larger wind turbines[1]. The small size of power converter, a cost efficient solution in order to obtain variable speed is one reason to increase DFIG uses more[2]. Many DFIG models are modeled in many papers[3-8], such as the full-model which is a 5th order model. Also in[6], the 3rd order model of DFIG is presented that uses a rotor current. By disregarding the stator flux linkage variations and given rotor voltage, the 3rd order model can be obtained[7-9]. Additionally, in order to model back-to-back converters in the simplest scenario, the converters are ideal and we have a constant DC-link voltage between the converters[7-13]. Therefore, a controllable voltage (current) source can be implemented, considering the converter control. Other similar papers are studied in[14-17]. However, while increasing during the fault condition, DC link voltage is not continuous. So, it is not possible to determine that the DFIG will mal-trip after a fault or not. However, as a hysteresis controller method it has two main disadvantages: non constant switching frequency while varying along the AC current; and secondly due to the severity and fortuitousness of the operation, the converter protection is troublesome[18]. A variable structure control (VSC) method for a DIFG is presented in[19], using the principles of an reactive and active power controller known as modified DPC and where VSC and space-vector modulation are combined to ensure better operation. The VSC technique is designed which provides robust power controls without frame transformation and the current controller that in the common control drive is used. In[20], a simulation model consisting of two DFIGs connected to IEEE 34-bus test for two vector control based method was set up to investigate the transient performance of the micro grid. Then, different types of faults of the DFIGs were analyzed through the simulation model by using vector control strategy. Also[21] focuses on the decoupled control of active and reactive power for variable speed constant frequency wind generation system and principle of maximum wind power tracking for wind generation system is analyzed. Also an effective method of independent active power and reactive power control is proposed. In[22] some control designs for a variable-speed constant-frequency wind energy system is presented using DFIG. This paper aim is to develop a nonlinear vector control technique using the second Lyapunov approach for the rotor side converter, and a network voltage vector control of the grid side converter, and to maximize the energy of the wind turbine and injected to the grid. In[23], the d-q model of the induction generator is developed from the fundamentals in a modular approach in Simulink and a fuzzy logic controller is designed for indirect vector control of induction generator. To provide a direct axis current reference I_d, which controls the motor flux, the speed control loop uses a fuzzy logic controller. The motor torque is controlled by Quad rature axis current reference I_d. Also in[24], a vector control technique is studied to control the rotor side voltage that allows the active and reactive power be controlled as well as the rotor speed in order to get the maximum wind power point. In fact a Neuro-fuzzy gain tuner is proposed to control the DFIG. Each Neuro-fuzzy system input is the generator speed error value, and active or reactive power. The choice of only one input simplifies the design of the system.

* Corresponding author:
hnabniki@ut.ac.ir (Hassan Abniki)
Published online at http://journal.sapub.org/ep

Under fault condition the DFIGs vector control is more significance. To resolve the problems, this paper proposes a DFIG vector control whereas sinusoidal PWM (SPWM) is applied to maintain the switching frequency constant. To get constant switching frequency, calculation of the required rotor voltage that must be supplied to the generator is adopted. The results show the appropriate performance of the presented method in all conditions.

2. Methodology

Nowadays variable speed wind methods have recently become very popular as generators. A more general scheme of the DFIG system with back-to-back converter is presented in[14] as shown in Fig. 1.

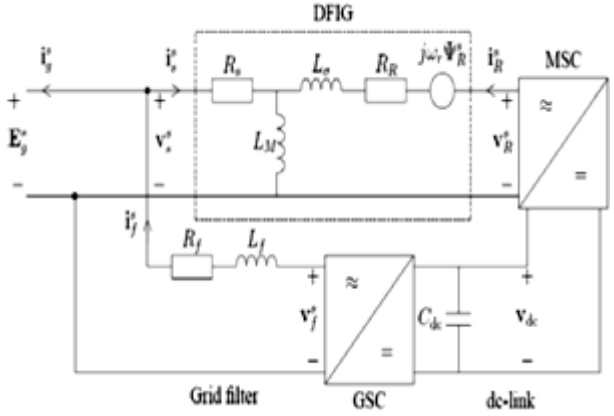

Figure 1. Equivalent circuit of the DFIG[14]

Equivalent circuit of the DFIG system of above model can be described by the following space vector equations:

$$V_S^s = R_s i_s^s + \frac{d\Psi_S^s}{dt} \quad (1)$$

$$V_R^s = R_R i_R^s + \frac{d\Psi_R^s}{dt} - jw_r \Psi_R^s \quad (2)$$

$$\Psi_s = L_M(i_s + i_R) \quad (3)$$

$$\Psi_R = (L_M + L_\sigma) i_R + L_M i_S = \Psi_S + L_\sigma i_R \quad (4)$$

$$T_e = 3n_p\, I_m[\Psi_S i_R^*] \quad (5)$$

where L_M is the magnetizing inductance, L_σ is the leakage inductance and n_p is the number of pole pairs. The total model of the DFIG system which presented in Fig. 1 can be summarized in synchronous coordinate equations as:

$$\frac{d\Psi_s}{dt} = E_g - R_S i_S + jw_1 \Psi_S \quad (6)$$

$$\frac{d\Psi_R}{dt} = V_R - R_R i_R + jw_2 \Psi_R \quad (7)$$

$$L_f \frac{di_f}{dt} = V_f - (R_f + jw_1 L_f) i_f - E_g \quad (8)$$

$$C_{dc} V_{dc} \frac{dV_{dc}}{dt} = -P_f - P_r \quad (9)$$

$$\frac{j}{n_p} \frac{dw_r}{dt} = T_e - T_s \quad (10)$$

$$\Psi_s = L_M(i_s + i_R) \quad (11)$$

$$\Psi_R = L_\sigma i_R + L_M(i_s + i_R) \quad (12)$$

$$T_e = 3n_p I_m[\Psi_S i_R^*] \quad (13)$$

$$P_r = 3R_e[V_R i_R^*] \quad (14)$$

$$P_f = 3I_m R_e[V_f i_f^*] \quad (15)$$

According to the equations 6 to 15, the stator voltage, V_s, has been changed to the grid voltage, E_g. Equations in stator rotating flux reference frame can be seen in[15]. Assuming x and y as horizontal and vertical axes of stator rotating flux reference frame, r_x and r_y as horizontal and vertical axes of rotor reference frame, S_D and S_Q as horizontal and vertical axes of stationary reference frame, stator flux angle and rotor angle can be obtained from equations 6 through 8. The next step is to calculate vertical and horizontal components of rotor and stator currents in stator rotating flux reference frame (equations 9 through 14).

$$\rho_S = tan^{-1}\left(\frac{\lambda_{SQ}}{\lambda_{SD}}\right) = tan^{-1}\left(\frac{i_{mSQ}}{i_{mSD}}\right) \quad (16)$$

$$i_{mSQ} = \left(\frac{L_S}{L_m}\right) i_{SQ} + i_{RQ} \quad (17)$$

$$i_{mSD} = \left(\frac{L_S}{L_m}\right) i_{SD} + i_{RD} \quad (18)$$

$$i_{rD} = i_{r\alpha}\ Cos(\theta_r) - i_{r\beta}\ Sin(\theta_r) \quad (19)$$

$$i_{rQ} = i_{r\beta}\ Sin(\theta_r) - i_{r\beta}\ Cos(\theta_r) \quad (20)$$

$$i_{rx} = i_{rD}\ Cos(\rho s) - i_{rQ}\ Sin(\rho s) \quad (21)$$

$$i_{ry} = -i_{rD}\ Sin(\rho s) + i_{rQ}\ Cos(\rho s) \quad (22)$$

$$i_{sx} = i_{sD}\ Cos(\rho s) + i_{sQ}\ Sin(\rho s) \quad (23)$$

$$i_{sy} = -i_{sD}\ Sin(\rho s) + i_{sQ}\ Cos(\rho s) \quad (24)$$

Vertical and horizontal components of linking flux are calculated in the new reference frame. Taking into account of this point in the new reference, the horizontal axis is adjusted to the stator linkage flux vector.

Thus, where V_d is the dc-link voltage, i_{os} is the current between the dc-link and the rotor, or i is the current between the dc-link and the stator, and C_d is the dc-link capacitor. Thus, the d –axis current i_{ds} is set by dc-link voltage controller and controls the active power flow between the utility gird and the dc-link. Finally, the strategy for the decoupled vector control of the grid side converter is shown in Fig. 2[16]. This control scheme has three control loops, one external loop to control the dc-link voltage and two internal loops to regulate the d–q current components, with the d-axis current component utilize to regulate the dc-link voltage and q-axis current component utilize to control the reactive power. The output slip power from DFIG and power factor of the grid can be controlled via changing d-axis current and q-axis current[16]. The control scheme of the rotor-side converter is organized in a generic way with two series of two PI controllers. Fig. 2(a) shows a schematic block diagram for the rotor-side converter control. The reference q-axis rotor current i_{rq}^* can be obtained either from an outer speed control loop or from a reference torque imposed on the machine. The flow of real and reactive power is controlled by the grid-side converter, through the grid interfacing inductance. The objective of the grid-side converter is to keep the dc-link voltage constant regardless of the magnitude and direction of the rotor power. The vector control method is used as well, enabling independent control of the active and reactive power flowing between the grid and the converter. The PWM converter with the d-axis current used to regulate the dc-link voltage and the q-axis current component to regulate the reactive power. Fig. 2(b) shows the schematic control structure of the grid-side

converter. Whole equations are available in[25] and also the abbreviations are as following:

$\vec{v}, \vec{i}, \vec{\varphi}$ Voltage, current and flux vectors

R_s, R_r Stator, rotor winding resistances

L_s, L_r, L_{ls}, L_{lr} Stator, rotor winding self- and leakage inductances

L_m Magnetizing inductance

w_s , w_r , w_{slip} Synchronous, rotor, slip angular frequency

P, Q Active and reactive power

s, r Stator and rotor subscripts

g Grid-side value subscripts

c Converter value subscripts

d, q d-axis and q-axis component subscripts

n Nominal value subscript

ref Reference value superscript

Regarding the equations in[15], and after a couple of other calculations, we have:

$$P_S = \frac{3}{2}(V_{sx} . i_{sx} + V_{sy} . i_{sy}) \quad (25)$$

$$Q_S = \frac{3}{2}(V_{sy} . i_{sx} + V_{sx} . i_{sx}) \quad (26)$$

Putting equations 19 and 22 then have:

$$P_S = -\frac{3}{2}|V_{sx}|\left(\frac{L_m}{L_s}\right) i_{ry} \quad (27)$$

$$Q_S = -\frac{3}{2}|V_s|\left(\frac{L_m}{L_s}\right)(i_{ms} - i_{rx}) \quad (28)$$

Noticing equations 25 and 26, the variations of vertical and horizontal components of rotor current in the new reference frame relates to stator power values, separate control of reactive and active power of DFIG possible, whereas p, q are the reactive and active power, respectively. For a system with $V_{qs} = 0$ which is used for the grid-connected converter, this simplifies the power equations to:

$$P = \frac{3}{2}(V_{ds} . i_{ds}) \quad (29)$$

$$Q = \frac{3}{2}(V_{ds} . i_{ds}) \quad (30)$$

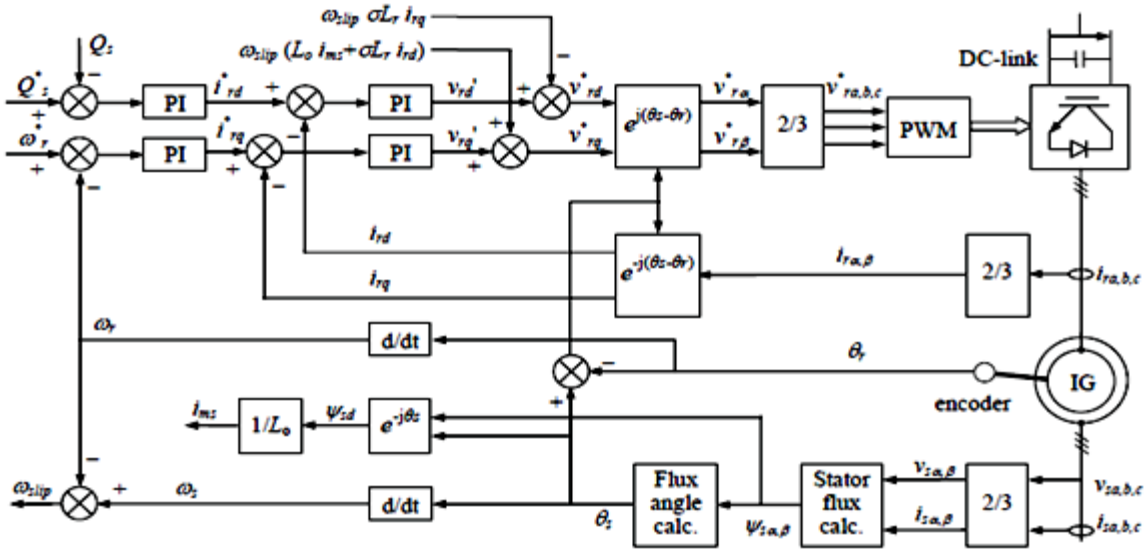

(a)

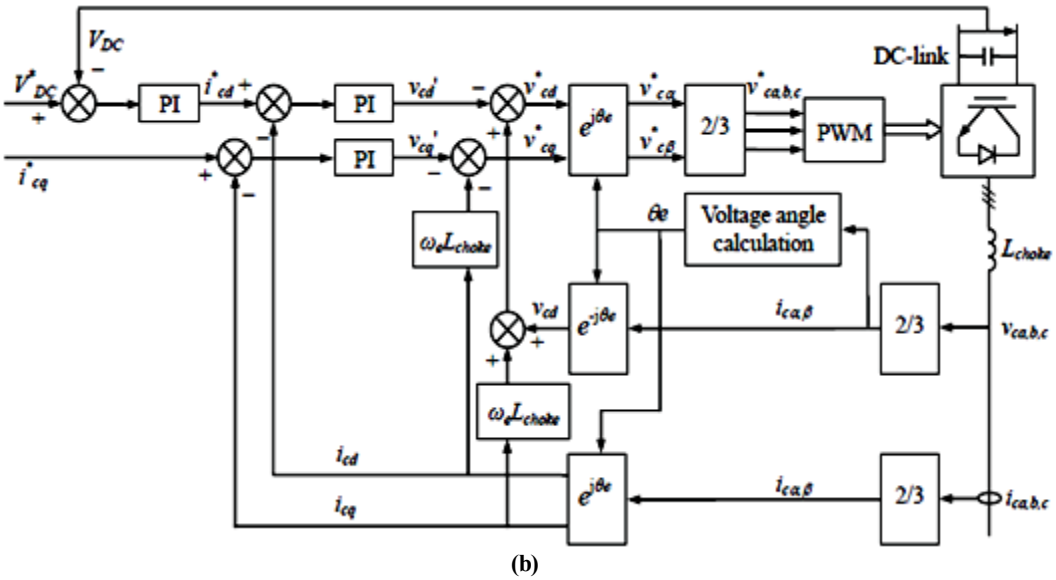

(b)

Figure 2. a) Vector control structure for rotor-side converter, b) Vector control scheme for grid-side converter[25]

From equation 12, the q -axis current is set to variable for reactive power control. The dc power has to be equal to the active power flowing between the utility grid and the dc-link inverter.

$$V_d . i_{OS} = \frac{3}{2}(V_{ds} . i_{ds}) \quad (31)$$

$$C_d \frac{dV_d}{dt} = i_{os} - i_{or} \quad (32)$$

3. Simulated Network

The stator of the wound rotor induction machine is connected to the low voltage balanced three phase grid and the rotor side is fed via the back-to-back IGBT voltage source inverters with a DC bus. the power flow is controlled by the front–end converter between the DC bus and the AC side and allows the system to be operated in sub-synchronous and super synchronous speed. Fig. 3 shows schematic of DFIG for wind turbine application and also Fig. 4 shows the schematic structure of DFIG application for the wind turbine simulated in PSCAD/EMTDC. In fact, DFIG is basically a standard rotor-wounded induction machine in which stator is directly connected to the grid. It can be said that converter has two parts: rotor-side, and grid-side. Rotor-side converter acts as a voltage source one, while the grid-side convertor is expected to keep the capacitor voltage under wind speed changes and different conditions of grid (Figs. 3 and 4).

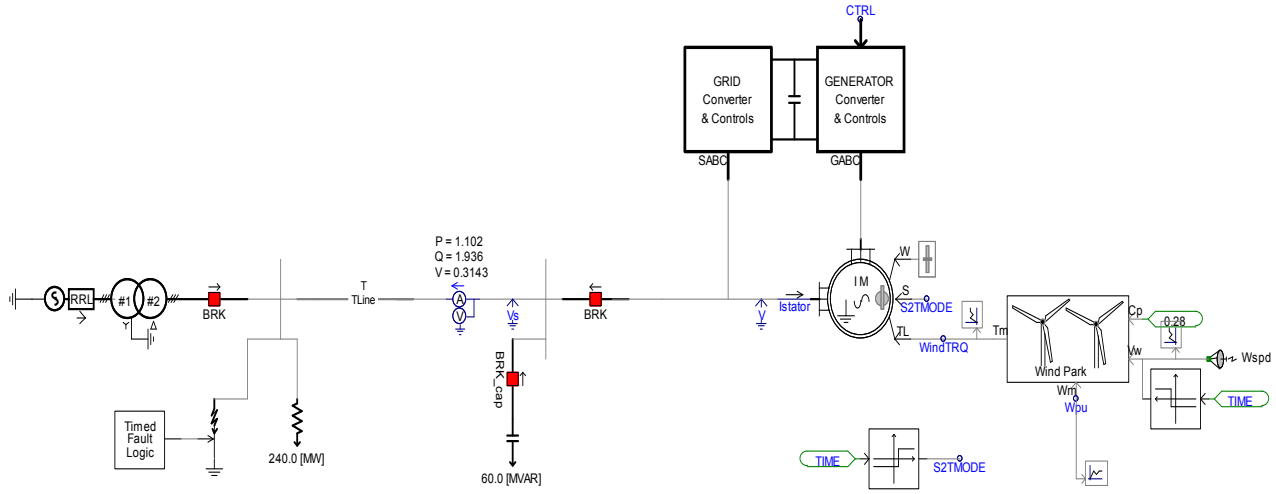

Figure 3. Schematic of simulated system by PSCAD/EMTDC

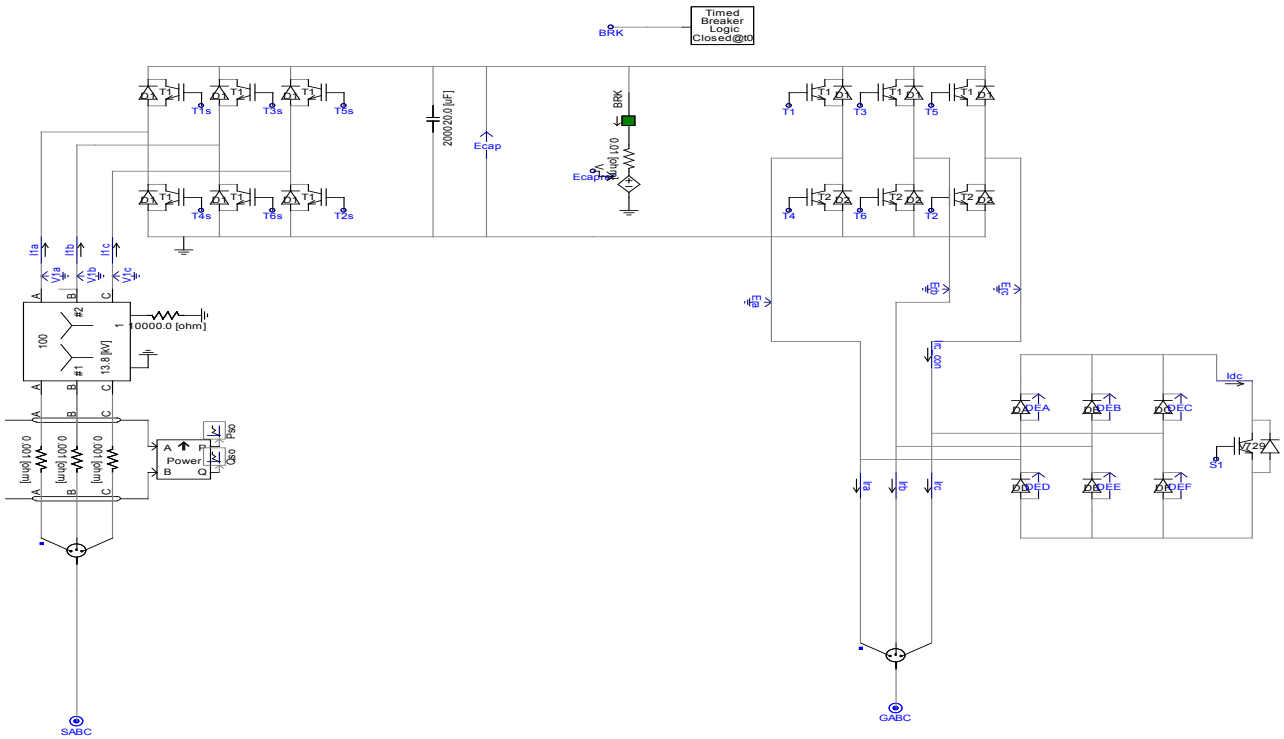

Figure 4. Schematic structure of inverter and rectifier simulated in PSCAD/EMTDC

The vector control strategy of the power converter is based on the stator flux field oriented control which both fundamental and harmonic currents are controlled. It is assumed that the total harmonic currents demanded by nonlinear loads connected to the utility are either sampled through current measurements. This makes the command harmonic currents for rotor side power converter[17]. The active power is generated regarding to wind speed and wind turbine characteristics while the reactive power command is set in regard to the utility demand. The rotor side power converter provides proper rotor excitation. In fact, the fundamental current controls the active and reactive powers. So, the utility current will be a sine wave. Decoupled control of the reactive and active powers and harmonic compensation are performed in this paper.

4. Results

The control scheme of the PSCAD/EMTDC simulated study case for a wind turbine utilizing DFIG was shown in previous section. The stator and rotor current waveforms of the induction generator are shown in Fig. 5. The case is set up to track for maximum wind power utilization. The 'power coefficient', C_p is a function of wind speed/machine speed. As wind speed a change, machine speed is changed to operate at maximum C_p , P and Q can be independently controlled irrespective of the machine slip (speed). Determining the relative difference between stator flux and rotor position is done for resolving the rotor currents. In all simulations, after 0.5 seconds, the control torque is applied. It is observed after 8th second, with a step change in speed, the flow rate have been retrieved. Also, in this paper using a filter, the stator flux dc component is removed. In Fig. 6, differences betrween stator and rotor flux of DFIG is shown. Also, Fig. 7 shows active and reactive and reference speed of DFIG. At time 8 sec, the reference speed changed and consequently the estimated speed changes. Also, active and reactive power changes whereas vector control do well this work as soon as possible in order to get maximum torque. Turbine speed and this difference are clearly seen in this view. The capacitor of dc link can be charged to amount of the charge. These capacitors are usually a great value. Diagram and the output converter voltage obtained are as following active and reactive power output of the reference speed and DFIG rotor speed that can be seen in the Fig. 8. In this Fig, after appliying verctor control at time 1 sec, some varions are inevitabe and after that maximum torque is reseulted. In Fig. 9 at time 3 sec, a fault was clearced while vector control was existed; so the variations are very little. Switching to torque control situation after 0.5 sec is done and untill this time, the machine rotate at a selected speed/sec as specified at the input W. This value is used as the initial speed. If a turbine start up is under investigation, then the initial value will have to be changed accordingly. Although, a step change in wind speed at the specified instant, this would cause the speed controller to react and maintain the tip speed ration for maximum power. In this regard, the optimal tip speed ration should be known and can be derived from the turbine torque equations.

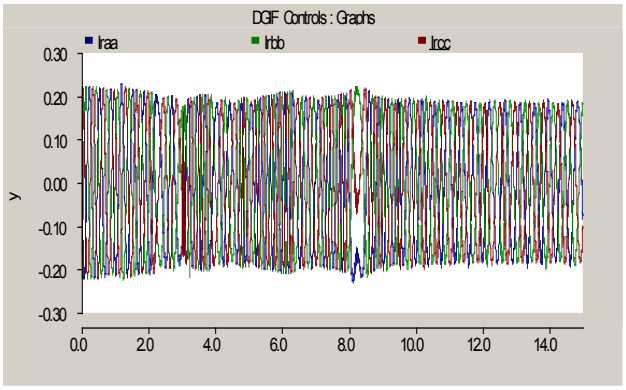

Figure 5. Turbine rotor current during speed variation

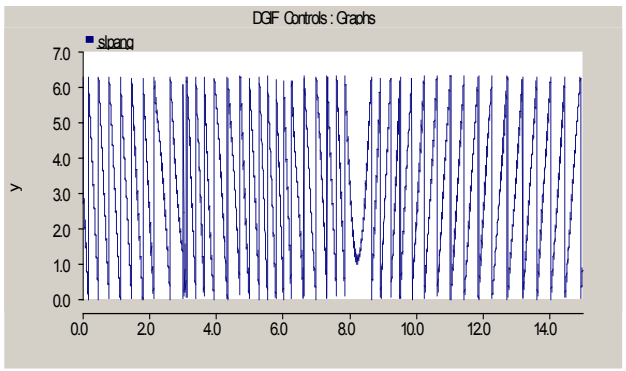

Figure 6. Differences betrween stator and rotor flux

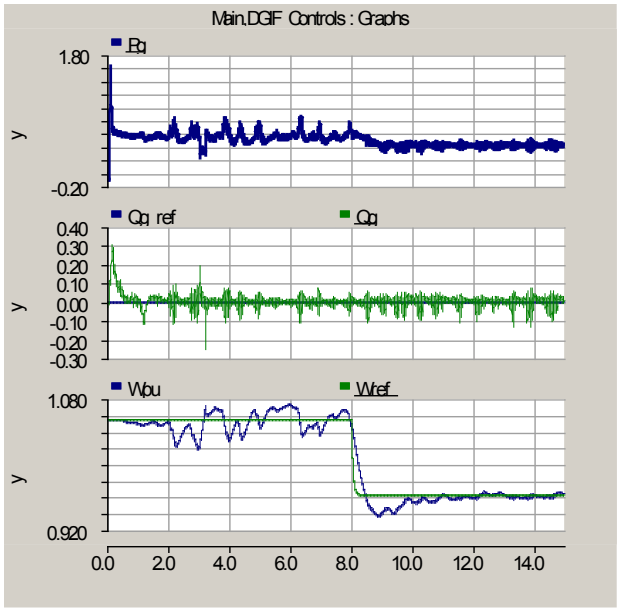

Figure 7. Active and reactive and referecne speed of DFIG

Tip speed ration will determine the value of Cp. (assumed constant in this example for simplicity).V_{dref1} is controlled by the capacitor voltage error. V_{qref1} is controlled by the stator side reactive power error (setting-actual). V_{dref1} and V_{qref1} are used to generate the stator side reference voltages for firing the switches (Fig. 8). The diagrams of reference voltage and

output two-axis wind turbine in the direction of *d* and *q* axis have shown in Fig. 9. The *rms* values of voltage and rotor current supposed as following:

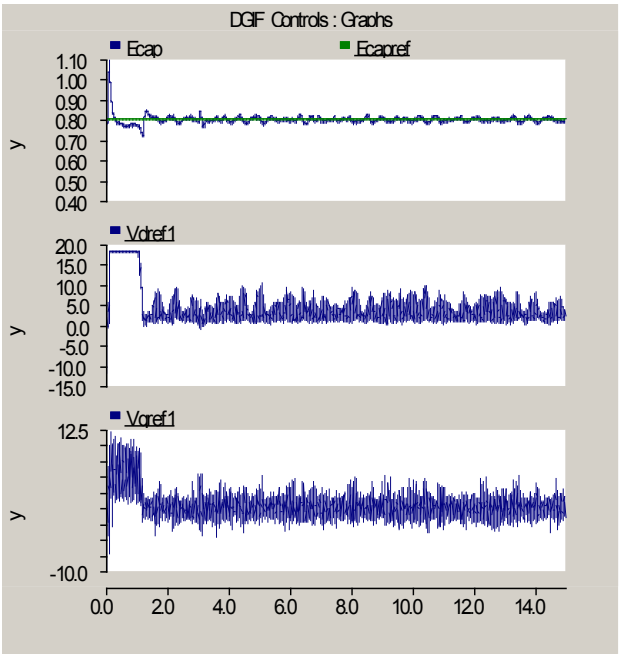

Figure 8. Reference voltage ouptputs for d and q axis of DFIG

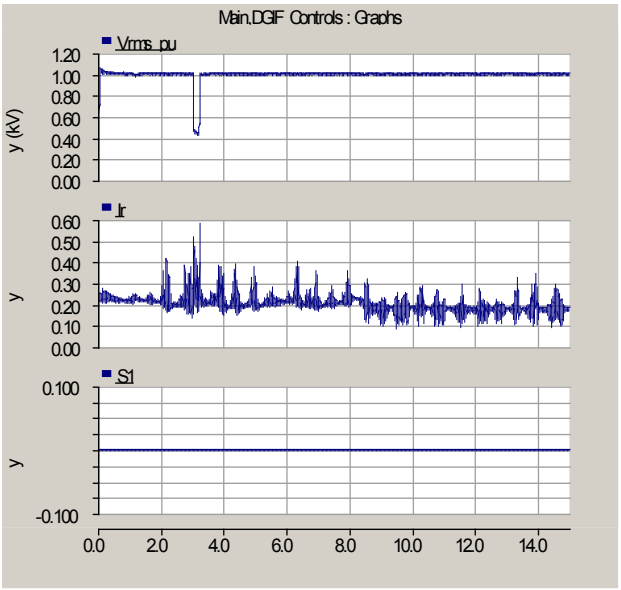

Figure 9. DFIG rotor current and voltage (rms) of DFIG

Initial wind speed is 12 m/s and the initial speed of machine is 1.1 pu. Identification of main stator flux by integrating stator voltage after removal of resistive drop.

The washout filter removes any dc component from the integrated flux without significantly effecting the phase. Block the rotor side inverter during the high enough rotor current to trigger the crowbar potection circuit, in fact when S_1=0, then crowbar will not be active (Fig. 9). Finally controlled current and voltage of DFIG can be seen, In fact, the axis *d*, the reactive power control model and the flow axis and *q*, the active power and control model that we have in this section will be controlled both simultaneously. The electrical and mechanical torque is seen in the Figs. 10 and 11. Also, *Tref* is the reference torque. In fact, Fig. 8 shows a simulation of the speed control loop with rated driving torque. In Fig. 11 at time 8 sec, reference speed is changed and consequently the torque changes as soon as possible by vector control. The produced voltages of DFIG can be seen in the Fig. 12. This figure shows the value of produced voltage for all phases and the *rms* value of produced voltage.

In this paper, the dynamic performance of the DFIG generator is shown. Also, during a 3 phase fault and step changes in load, it is found that similar to previous sections initially generator operates at essentially rated condition with a load torque to base torque. Similarly, Figs. 12 (a, and b) also show the voltage and the current waveforms of the converter operating in the inverting mode when a fault happens at 3 sec. In addition, dynamic performances of wind turbine with DFIG and dc machine coupled with DFIG are some different transient conditions because of dc machine have different time constant.

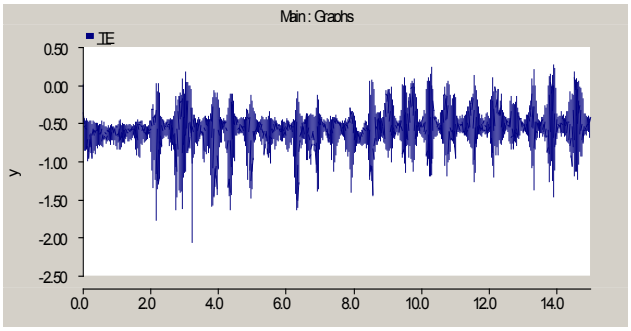

Figure 10. Electrical torque of DFIG

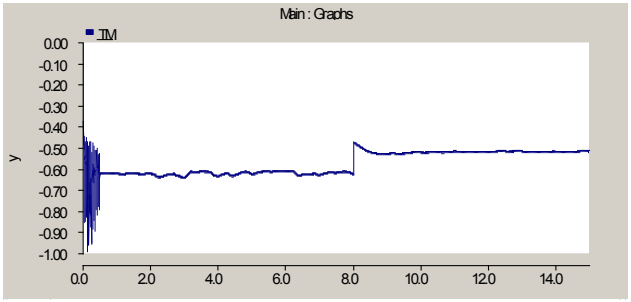

Figure 11. Mechanical torque of DFIG

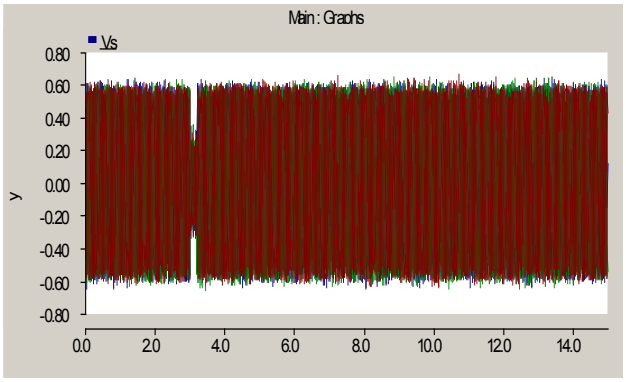

(a)

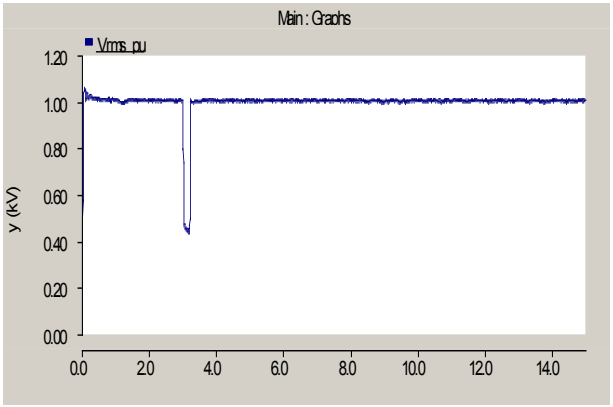

(b)

Figure 12. a) The value of produced voltage for all phases, b) The *rms* value of produced voltage

5. Conclusions

In this paper, a doubly fed induction generator as the power conversion system in wind turbines is analysed by vector controlled for better control of the grid while injecting the required active power of the system. The system model is developed in the dedicated power electronics and system simulation tool, EMTDC software. The model includes wind speed fluctuations, enabling simulation of the power quality characteristics of the wind turbine. Based on results, the proposed vector control of DFIG is capable of simultaneous capturing maximum power of wind energy with fluctuating wind speed and improving power quality, and this is achieved by cancelling the most significant and troublesome harmonics of the utility grid by vector control. Reactive and active power controls are the other two significant features of the proposed technology. Also, vector control of DFIG wind turbines is investigated after the clearance of short circuit faults in grid.

REFERENCES

[1] T. Ackermann, L. Soder, "An overview of wind energy-status," *Renewable and Sustainable Energy Reviews*, vol. 6, no. 1/2, pp. 67-127, 2002.

[2] L. H. Hansen, P. H. Madsen, F. Blaabjerg, H. C. Christensen, U. Lindhard, K. Eskildsen, "Generators and power electronics technology for wind turbines," *Proc. of the 27th Annual Conference of the IEEE on Industrial Electronics Society*, vol. 3, pp. 2000-2005, Nov 2001.

[3] T. Sun, Z. Chen, F. Blaabjerg, "Transient analysis of grid-connected wind turbines with DFIG after an external short circuit fault,"*4th Nordic wind power conference*, *Chalmers University of Technology*, Sweden, 2004.

[4] R. Koessler, S. Pillutla, L. Trinh, "Integration of large wind farms into utility grids (Part 1-Modeling of DFIG)," *IEEE Power Engineering Society general meeting*, Toronto, Canada, 2003.

[5] P. Pourbeik, R. Koessler, D. Dickmander, "Integration of wind farms into utility grids (Part 2)," *IEEE Power Engineering Society general meeting,* Toronto, Canada, 2003.

[6] Y. Kazakchov, J. Feltes, R. Zavadil, "Modeling wind farms for power system stability studies," *IEEE Power Engineering Society General Meeting*, vol. 3, July 2003.

[7] L. Holdsworth, X. Wu, N. Jenkins, "Dynamic modeling of doubly fed induction generator wind turbines," *IEEE Transaction on Power Systems*, vol. 2, pp. 803-809, 2003.

[8] L. Holdsworth, J. Ekanayake, N. Jenkins, "Comparison of fixed speed and doubly-fed induction wind turbines during power system disturbances," *IEE Proceedings of Generation, Transmission, Distribution*, vol. 3, no.3 , pp. 343-352, 2003.

[9] A. Feijoo, J. Cidaras, C. Carrillo, "A third order model for the doubly-fed induction machine," *Electric Power Systems Research Journal,* vol. 3, pp.26-33, 2002.

[10] J. Slootwe, H. Polinder, W. Klin, "Dynamic modeling of a wind turbine with doubly fed induction generator," *IEEE Power Engineering Summer Meeting*, Vancouver, Canada. 2001.

[11] J. Rodriguez, "Incidence on power system dynamics of high penetration of fixed speed and doubly fed wind energy systems, study of the Spanish case," *IEEE Transaction on Power Systems*, vol. 4, pp.1089-1095, 2002.

[12] T. Thiringer, A. Peterson, T. Petru, "Grid disturbance response of wind turbines equipped with induction generator and doubly-fed induction generator," *IEEE Power Engineering Society General Meeting*, Toronto, Canada, 2003.

[13] A. Tapia, G. Tapia, J. Ostolaza, J. Saenz, "Modeling and control of a wind turbine driven doubly fed induction Generator," *IEEE Transaction on Energy Conversion*, vol. 2, pp. 194-204, 2003.

[14] V. Spoiala, H. Silaghi, D. Spoiala, "Control of doubly-fed induction generator system for wind turbines," *International Conference on Electric Machines and Drives,* pp. 1936 – 1941, 2005.

[15] A. Abedi, M. Pishvaei, A. Madadi, H. Meshgin, "Analyzing vector control of a grid-connected DFIG under simultaneous changes of two inputs of control system," *European Journal of Scientific Research*, vol. 45, no. 2, pp.221-231, 2010.

[16] W. Srirattanawichaikul, Y. Kumsuwan, S. Premrudeepreech acharn, B. Wu, "A vector control of a grid-connected 3L-NPC-VSC with DFIG drives," *International Conference on Electrical Engineering/Electronics Computer Telecommunications and Information Technology (ECTI-CON),* pp. 828 – 832, 2010.

[17] F.Shahnia1,B. Mohammad,B.Sharifian,"PSCAD/EMTDC based simulation of double fed induction generator for wind turbines," *Industrial Power System Modeling and Simulation Using PSCAD*, Korea University, Korea, 2005.

[18] M. Kazmierkowsk, R. Krishnan, F. Blaabjer, "Control in Power Electronics," *Academic press*, 2001.

[19] C. Dongkyoung, L. Kyo-Beum, "Variable structure control of the active and reactive powers for a DFIG in wind turbines", *IEEE Transactions on Industry Applications*, vol. 46, Issue. 6, pp. 2545 – 2555, 2010.

[20] M. Chen, L. Yu, N.S. Wade, L. Xiaoqin, L, Qing, Y. Fan, "Investigation on the faulty state of DFIG in a micro grid", *IEEE Transactions on Power Electronics*, vol. 26 , Issue. 7, pp.1913 – 1919, 2011.

[21] L. Donghui, L. Lei, "Research on active and reactive power's decoupled control strategy of the AC exited VSCF wind generation system," *International Conference on Electric Information and Control Engineering (ICEICE)*, pp. 3490 – 3493, 2011.

[22] J. B. Alaya, A Khedher, M. F. Mimouni, "Nonlinear vector control strategy applied to a variable speed DFIG generation system", *8th International Multi-Conference on Systems, Signals and Devices (SSD)*, pp. 1 – 8, 2011.

[23] Y. S. Rao, A. J. Laxmi, "Fuzzy logic based indirect vector control of induction generator in wind energy conversion system", *International Conference on Power, Signals, Controls and Computation (EPSCICON)*, pp.1 – 5, 2012.

[24] H. M. Jabr, L. Dongyun; N.C. Kar, "Design and Implementation of Neuro-Fuzzy vector control for wind-driven doubly-fed induction generator", *IEEE Transactions on Sustainable Energy*, vol. 2 , Issue. 4, pp. 404 – 413, 2011.

[25] J. Fletcher, J. Yang, "Introduction to Doubly-Fed Induction Generator", *University of Strathclyde, Glasgow United Kingdom for Wind Power Applications*.